Fast Simulation of Electromagnetic Field Propagation through Multiple Non-parallel Planar Surfaces

Site Zhang*, Christian Hellmann**, Frank Wyrowski*
*Applied Computational Optics Group, Friedrich Schiller University Jena
**Wyrowski Photonics UG, Jena
mailto:site.zhang@uni-jena.de

By investigating the propagation of electromagnetic fields through a sequence of planar surfaces in the spatial frequency domain, it is found that the spatial frequencies are independent from one another. From that we conclude a straight-forward algebraic operation and also implemented an efficient numerical algorithm.

1 Introduction

Various optical components can be modeled as a sequence of planar surfaces and the homogeneous media in between, such as prisms. To model electromagnetic fields propagation through such components, one must deal with 1) the transmission/reflection at each planar surface, and 2) the propagation in the homogeneous regions between adjacent, and in general, non-parallel surfaces. The two issues, although have been studied as separate topics, the efficient use of them in combination, especially in the case with multiple surfaces, has not been discussed in depth. We investigate it as a whole in the spatial frequency domain (k-domain), in which we show that the spatial frequencies are independent from one another. As a consequence, a great numerical advantage can be obtained, because the number of the spatial frequencies used in the simulation can be varied without influencing each other.

2 Theory

The situation under consideration is depicted in Fig. 1, and the case of sequential propagation through these surfaces is taken as an example (it is possible to handle non-sequential processes too).

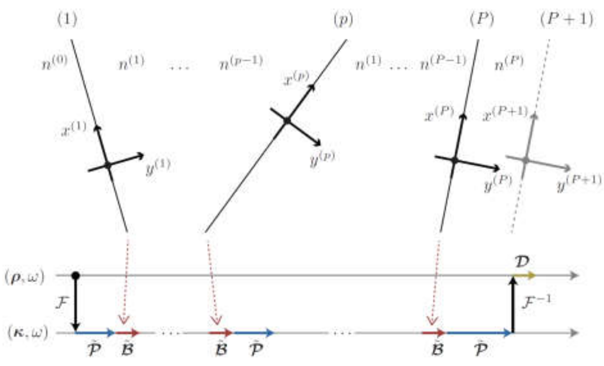

Fig. 1 Multiple planar surfaces with the corresponding coordinate systems $x^{(p)}-y^{(p)}-z^{(p)}$ and media with refractive index $n^{(p)}$ in between.

Our treatment of the whole propagation process can be explained with the field tracing diagram [1] shown on the lower part of Fig. 1: the input field defined in the spatial domain is first transformed to the k-domain by a Fourier transform $\mathcal{F}$; then, a series of propagation operators $\tilde{\mathcal{P}}$ and interface operators $\tilde{\mathcal{B}}$ are applied; finally, the result in k-domain can be transformed back to the spatial domain by $\mathcal{F}^{-1}$ for further analysis by the detector $\mathcal{D}$. It is worth mentioning that the Fourier transform and its inverse can be evaluated by the semi-analytical approach [2] or the geometric one [1] for better numerical performance in comparison to the standard FFT.

The propagation $\tilde{\mathcal{P}}$ between two non-parallel surfaces as in Fig. 1 can be handled as follows. The first step is to map the variables in k-domain, using the relation below

$$
\begin{aligned}
k_x^{(p+1)} &= a_{11}^{(p,p+1)} k_x^{(p)} + a_{12}^{(p,p+1)} k_y^{(p)} + a_{13}^{(p,p+1)} k_z^{(p)}\,, \\
k_y^{(p+1)} &= a_{21}^{(p,p+1)} k_x^{(p)} + a_{22}^{(p,p+1)} k_y^{(p)} + a_{23}^{(p,p+1)} k_z^{(p)}\,,
\end{aligned}
\tag{1}
$$

with $a_{ij}^{(p,p+1)}$ as the elements of the rotation matrix from (p) to $(p+1)$. Since each planar surface is labelled with an unique index (p), we will directly define the associated coordinate Cartesian system as $x^{(p)}-y^{(p)}-z^{(p)}$, and $k_x^{(p)}-k_y^{(p)}-k_z^{(p)}$ in k-domain. The next step is to find the changes in field amplitudes during the propagation. As is shown in [3], it can be summarized as

$$
\tilde{\boldsymbol{E}}_\perp^{<(p+1)} = \left|\underline{\boldsymbol{J}}^{(p,p+1)}\right| \exp\left(\mathrm{i}\zeta^{(p,p+1)}\right) \underline{\boldsymbol{q}}^{(p,p+1)} \tilde{\boldsymbol{E}}_\perp^{>(p)}\,,
\tag{2}
$$

with $\tilde{\boldsymbol{E}}_\perp := (\tilde{E}_x, \tilde{E}_y)$ defined as the angular spectrum on the transverse plane, and with "<" / ">" to indicate the left / right side of the surface; $\underline{\boldsymbol{J}}^{(p,p+1)}$ is the Jacobian matrix that describes the ratio between the integration interval area in the $k_x^{(p)}-k_y^{(p)}$ plane and that in the $k_x^{(p+1)}-k_y^{(p+1)}$ plane; the term ζ is a result of the translation between two coordinate systems (without rotation considered), and it is defined as

$$\zeta = k_x^{(p)}\Delta x^{(p,p+1)} + k_y^{(p)}\Delta y^{(p,p+1)} + k_z^{(p)}\Delta z^{(p,p+1)} \,. \tag{3}$$

The 2×2 matrix $\underline{\boldsymbol{q}}^{(p,p+1)}$ describes the projection of the field components from one coordinate system to another, and its elements are defined as

$$\begin{aligned} q_{11}^{(p,p+1)} &= a_{11}^{(p,p+1)} - a_{13}^{(p,p+1)} k_x^{(p)}/k_z^{(p)} \,, \\ q_{12}^{(p,p+1)} &= a_{12}^{(p,p+1)} - a_{13}^{(p,p+1)} k_y^{(p)}/k_z^{(p)} \,, \\ q_{21}^{(p,p+1)} &= a_{21}^{(p,p+1)} - a_{23}^{(p,p+1)} k_x^{(p)}/k_z^{(p)} \,, \\ q_{22}^{(p,p+1)} &= a_{22}^{(p,p+1)} - a_{23}^{(p,p+1)} k_y^{(p)}/k_z^{(p)} \,. \end{aligned} \tag{4}$$

The transmission / reflection operator $\tilde{\boldsymbol{\mathcal{B}}}$ at a planar surface can be expressed as (here we take transmission as an example)

$$\tilde{\boldsymbol{E}}_\perp^{>(p)} = \underline{\boldsymbol{T}}^{(p)} \tilde{\boldsymbol{E}}_\perp^{<(p)} \,. \tag{5}$$

Because the k_x- and k_y-components are always conserved on a planar surface, there is no changes in these variables in the process described above. The transmission coefficients $\underline{\boldsymbol{T}}$ can be efficiently calculated with the S-matrix method [4].

By using Eq. (2) and (5) in combination and repeating them, the whole propagation process through multiple surfaces can be written down till any position, e.g., in front of surface $(P+1)$, as

$$\begin{aligned} \tilde{\boldsymbol{E}}_\perp^{<(P+1)} = \prod_{p=1}^{P} \Bigg[\left| \underline{\boldsymbol{J}}^{(p,p+1)} \right| \exp\left(\mathrm{i}\zeta^{(p,p+1)}\right) \\ \times \underline{\boldsymbol{q}}^{(p,p+1)} \underline{\boldsymbol{T}}^{(p)} \Bigg] \tilde{\boldsymbol{E}}_\perp^{<(1)} \,. \end{aligned} \tag{6}$$

Let us further examine the term $|\underline{\boldsymbol{J}}|$ explicitly, and it is possible to find out the following conclusion

$$\begin{aligned} \prod_{p=1}^{P} \left| \underline{\boldsymbol{J}}^{(p,p+1)} \right| &= \prod_{p=1}^{P} \frac{\delta A^{(p)}}{\delta A^{(p+1)}} \\ &= \frac{\delta A^{(1)}}{\delta A^{(2)}} \frac{\delta A^{(2)}}{\delta A^{(3)}} \cdots \frac{\delta A^{(P)}}{\delta A^{(P+1)}} = \frac{\delta A^{(1)}}{\delta A^{(P+1)}} \,. \end{aligned} \tag{7}$$

Substituting the result in Eq. (7) back to Eq. (6), we obtain

$$\begin{aligned} \tilde{\boldsymbol{E}}_\perp^{<(P+1)} = & \frac{\delta A^{(1)}}{\delta A^{(P+1)}} \exp\left(\mathrm{i} \sum_{p=1}^{P} \zeta^{(p,p+1)}\right) \\ & \times \prod_{p=1}^{P} \left[\underline{\boldsymbol{q}}^{(p,p+1)} \underline{\boldsymbol{T}}^{(p)} \right] \tilde{\boldsymbol{E}}_\perp^{<(1)} \,. \end{aligned} \tag{8}$$

Eq. (8) implies a straight-forward numerical routine: a series of matrix multiplications in the last term within the brackets; an exponential term that summarizes the translational relations between coordinate systems; and the term $[\delta A^{(1)}/\delta A^{(P+1)}]$, which can be regarded as a scaling factor between the first surface (1) and the last one $(P+1)$. The numerical calculation of the scaling factors plays an important role determining the overall efficiency, because the handling of non-equidistant grid is involved [3]. By reducing the number of such calculations to only once as in Eq. (8), we can greatly improve the numerical performance in comparison to Eq. (6).

3 Example

We implemented a numerical algorithm following Eq. (8), and applied it to the example as in Fig. 2. A convergent spherical wave is used as the input, with a wavelength of 532 nm, truncated to a diameter of 750 µm, and linearly polarized along x-direction. It is supposed to focus after a distance of 15 mm in free space.

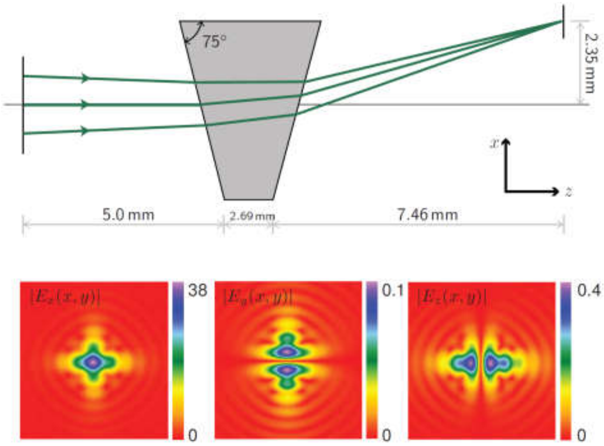

Fig. 2 *Propagation of a congergent spherical wave through a prism. The medium of the prism has the refractive index of 1.5 at the wavelength of* 532 nm*, while the surrouding medium is vacuum.*

After being deflected by the prism, the amplitudes of three electric field components at a shifted focal plane along x-direction, as in the lower part of Fig. 2. The simulation takes the vectorial effects at each interfaces into consideration, as well as the diffraction effects due to the truncation of the field size and the focusing.

References

[1] F. Wyrowski, “Physical optics modeling,” Friedrich Schiller University Jena, 2017 Summer, Lecture.

[2] Z. Wang, “Analytical handling of optical wavefront,” Friedrich Schiller University Jena, 2015, Master thesis.

[3] S. Zhang, D. Asoubar, C. Hellmann, and F. Wyrowski, “Propagation of electromagnetic fields between non-parallel planes: a fully vectorial formulation and an efficient implementation,” Appl. Opt. **55**, 529-538 (2016)

[4] L. Li, “Note on the S-matrix propagation algorithm,” J. Opt. Soc. Am. A **20**, 655-660 (2003).